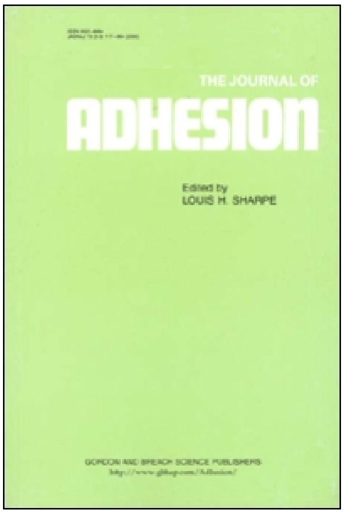


**The Journal of Adhesion**
Publication details, including instructions for authors and subscription information:
http://www.informaworld.com/smpp/title~content=t713453635

# Strength Analysis of Adhesively-Bonded Tubular Single Lap Steel-Steel Joints Under Axial Loads Considering Residual Thermal Stresses

Young Goo Kim[a]; Su Jeong Lee[ab]; Dai Gil Lee[a]; Kwang Seop Jeong[c]
[a] Design Lab. with Advanced Materials, Department of Mechanical Engineering, Korea Advanced Institute of Science and Technology, Taejon-shi, Korea [b] Currently Samsung Elec. Co. Ltd., [c] Department of Textile Engineering, Yeung-Nam University, Kyung-buk, Korea

**To cite this Article** Kim, Young Goo , Lee, Su Jeong , Lee, Dai Gil and Jeong, Kwang Seop(1997) 'Strength Analysis of Adhesively-Bonded Tubular Single Lap Steel-Steel Joints Under Axial Loads Considering Residual Thermal Stresses', The Journal of Adhesion, 60: 1, 125 — 140

**To link to this Article: DOI:** 10.1080/00218469708014414

**URL:** http://dx.doi.org/10.1080/00218469708014414

*J. Adhesion*, 1997, Vol. 60, pp. 125–140
Reprints available directly from the publisher
Photocopying permitted by license only



# Strength Analysis of Adhesively-Bonded Tubular Single Lap Steel-Steel Joints Under Axial Loads Considering Residual Thermal Stresses

YOUNG GOO KIM, SU JEONG LEE*, DAI GIL LEE

*Design Lab. with Advanced Materials, Department of Mechanical Engineering, Korea Advanced Institute of Science and Technology, Kusong-dong, Yusung-gu, Taejon-shi, 305-701, Korea*

and

KWANG SEOP JEONG

*Department of Textile Engineering, Yeung-Nam University, Dae-dong, Kyungsan-shi, Kyung-buk, 712-749, Korea*



*(Received November 16, 1995; in final form March 7, 1996)*

The static tensile load bearing capability of adhesively-bonded tubular single lap joints calculated using linear mechanical adhesive properties is usually far less than the experimentally-determined one because the majority of the load transfer of adhesively-bonded joints is accomplished by the nonlinear behavior of the rubber-toughened epoxy adhesive

In this paper, both the nonlinear mechanical properties and the residual thermal stresses in the adhesive resulting from joint fabrication were included in the stress calculation of adhesively-bonded joints. The nonlinear tensile properties of the adhesive were approximated by an exponential equation which was represented by the initial tensile modulus and ultimate tensile strength of the adhesive.

From the tensile tests and the stress analyses of adhesively-bonded joints, a failure model for adhesively-bonded tubular single lap joints under axial loads was proposed.

KEY WORDS: Adhesively bonded tubular single lap joint; nonlinear mechanical property; tensile load bearing capability; linear approximation; nonlinear exponential approximation; residual thermal stress; failure criterion.

## INTRODUCTION

The design of joints for the assembly of the separated parts of structures has become an important research area because the structural efficiency of a structure with joints is established, with very few exceptions, by its joints and not by its basic structure.

There are two main types of joints: mechanical and adhesively-bonded. (There are, of course, also welded joints). The mechanical joint is created by fastening the

*Currently Samsung Elec. Co. Ltd.

substrates with bolts or rivets, but the adhesively-bonded joint uses an adhesive interlayer between the adherends.

The adhesively-bonded joint can distribute load over a larger area than the mechanical joint, requires no holes, adds very little weight to the structure and has superior fatigue resistance.[1,2] However, the adhesively-bonded joint requires careful surface preparation of the adherends, is affected by service environments and difficult to disassemble for inspection and repair.

There are several types of tubular lap joints, such as the single lap joint, the double lap joint, the stepped lap joint, and the scarf lap joint. From these, the tubular single lap joint is most popular, due to its ease of manufacture and its relatively low cost.

Stress analyses of adhesively-bonded tubular single lap joints under axial load have been conducted by a few researchers through analytical and finite element methods.[3-9] Rubkin and Reissner[3] assumed that the adhesive thickness was much smaller than the adherend thickness and that the adherend thickness was much smaller than the radius of the tubular joint, from which they applied thin shell theory to the joint analysis. They modelled the adhesive layer as an infinite number of coil springs with the assumption that the adhesive was much softer than the adherend. Adams and Peppiatt[4] refined the solution of Volkersen and gave a closed-form solution for the shear stresses of the adhesively-bonded tubular single lap and partially-tapered tubular scarf lap joints. They also analyzed adhesively-bonded tubular single lap joints which were subjected to axial and torsional loads using the finite element method when the adhesive had a fillet. Griffin *et al.*[5] proposed a strength model which could predict the fracture of the adhesively-bonded single lap joint under tensile loads. Shi and Cheng[6] proposed an approximate closed form solution for the stress distributions in the adhesive and adherends when the adhesively bonded lap joints were under tensile loads. Terekhova and Skoryi[7] proposed the closed form solution for adhesively-bonded lap joints under tensile loads and internal pressure. They applied thin shell theory to the joint analysis. Kukovyakin and Skoryi[8] proposed a closed form solution for an adhesively-bonded bush-shaft type joint under tensile loads. They considered that the bushes were thin-walled and deformed in accordance with the moment theory of thin-walled shells. Harrison and Harrison[9] developed a simple method for calculating the stresses near the ends of a parallel-sided adhesive layer.

In the majority of the past works, the linear elastic shear properties of the adhesive have been used in the stress analysis of the adhesively-bonded tubular single lap joint. However, the adhesive under load usually experiences large plastic deformation before the onset of adhesive fracture and, consequently, the majority of the load transfer of the adhesively-bonded joint is accomplished by the nonlinear plastic behavior region of the adhesive.[10] If the nonlinear properties of the adhesive are included, complicated mathematics and long computational time are required for the analysis.[11]

In this paper, the nonlinear mechanical properties of the adhesive were taken into consideration in the stress analyses of adhesively-bonded tubular single lap joints with steel-steel adherends. The nonlinear tensile stress-strain relationship of the adhesive was modelled by a two-parameter exponential equation that was represented by the initial tensile modulus and ultimate tensile strength of the adhesive. The initial tensile modulus and ultimate tensile strength of the adhesive can be obtained by the tensile test.

In this work, the tensile load-bearing capabilities of adhesive joints were experimentally obtained. Then the stress distributions in the adhesive of adhesively-bonded tubular single lap joints were obtained by applying the measured tensile load-bearing capabilities. The stress distributions were calculated in four different cases: (case 1) nonlinear mechanical property with residual thermal stresses of the adhesive, (case 2) linear mechanical property with residual thermal stresses of the adhesive, (case 3) nonlinear mechanical property without residual thermal stresses of the adhesive, (case 4) linear mechanical property without residual thermal stresses of the adhesive.

From the experimental data, and the results obtained from the stress analyses, a failure model for the adhesively-bonded tubular single lap joints with steel-steel adherends under axial loads was proposed.

## EXPERIMENTS

The closed form solution as well as the finite element calculation predicted that the load-bearing capability of the adhesively-bonded joint increased as the adhesive thickness increased, which is contrary to the experimental result. In reality, the load-bearing capability of the adhesively-bonded joint decreases as the adhesive thickness increases because the residual thermal stresses from fabrication, originating from the cure of the adhesive, lowers the fracture strength of the adhesive.

In this work, the adhesively-bonded tubular single lap joints with steel-steel adherends under axial tensile load were measured to investigate the tensile load bearing capabilities with respect to adhesive thickness.

Figure 1 shows the adhesively-bonded tubular single lap joint with steel-steel adherends.

The thickness of the joint was adjusted by changing the outer diameter of the inner adherend while the inner diameter of the outer adherend was fixed. The outer



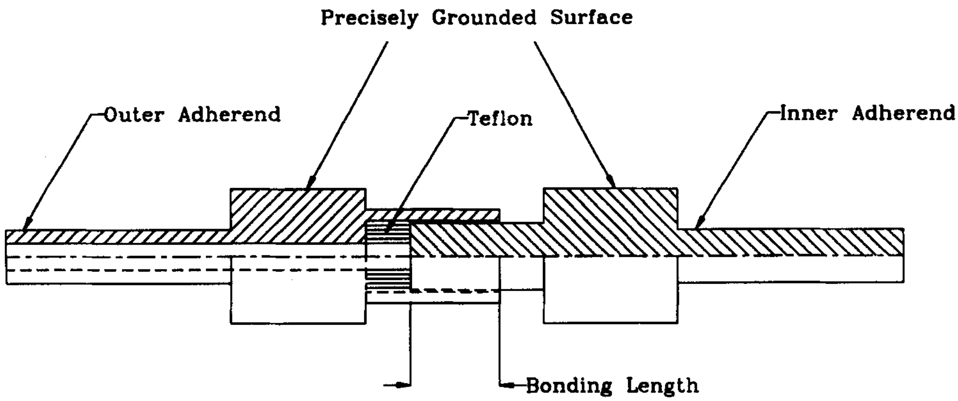


FIGURE 1 Configuration of the adhesively-bonded joint specimen.

and inner diameters of the outer adherend were 21 mm and 17 mm, respectively. The tensile load bearing capabilities of the joints were measured when the adhesive thickness varied from 0.05 mm to 1.0 mm.

Both the inner and outer adherends have precisely ground surfaces which were mounted on a precise V-block during the cure of the adhesive for concentric bonding. An arithmetic surface roughness of 2 μm was chosen for the adherend surface roughness because this value had proven to be the optimum for the fatigue strength of the adhesively-bonded tubular single lap joint.[12] The adhesively-bonded joints were cured in an autoclave for 4 hours under a temperature of 80°C and a pressure of 0.6 MPa.

Figure 2 shows the experimentally obtained tensile load-bearing capabilities with the curve fitting line when the bonding length was 20 mm. As shown in Figure 2, the tensile load-bearing capabilities of the adhesively-bonded joints decreased as the adhesive thickness increased. This is a similar phenomenon to the torque-bearing capabilities of the adhesively-bonded tubular joints with respect to the adhesive thickness.[13] Therefore, it is necessary to take into consideration of the residual



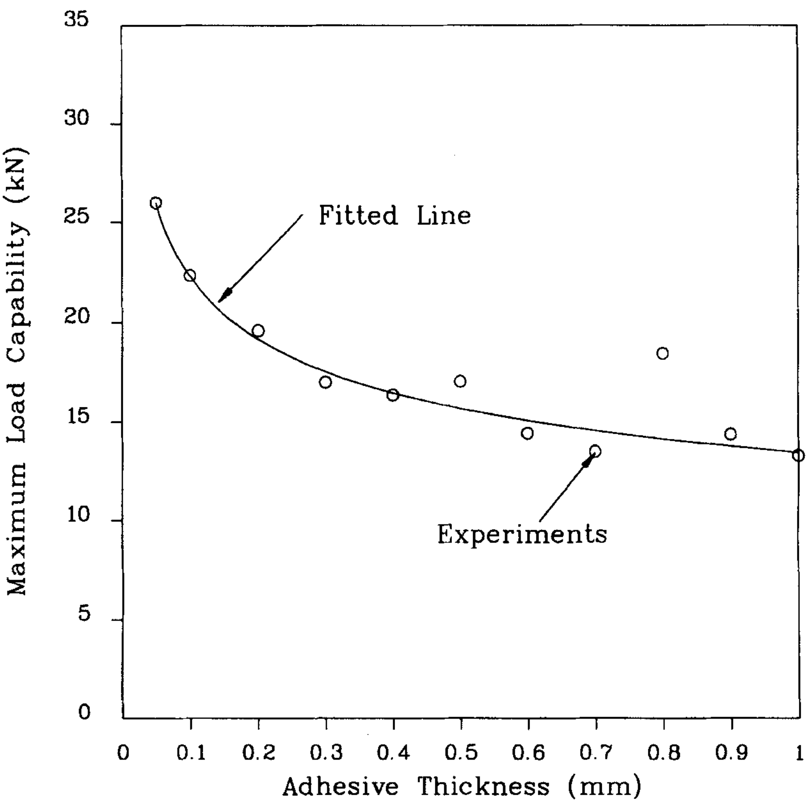


FIGURE 2 Static load capability of the adhesively-bonded tubular single lap joint.

thermal stresses in the adhesive resulting from joint fabrication for the better prediction of the static tensile load-bearing capability of the adhesively-bonded tubular single lap joint.

## NONLINEAR BEHAVIOR OF THE RUBBER-TOUGHENED ADHESIVE

The adhesive used in this work was IPCO 9923 rubber-toughened epoxy manufactured by the Imperial Polychemicals Corporation (Azusa, California, USA) which had high shear and peel strengths. Table I shows the material properties of the adhesive.

The nonlinear mechanical properties of the adhesive were modelled by the following exponential form.

$$\sigma = \sigma_m \left(1 - e^{-\frac{E}{\sigma_m}\varepsilon}\right) \tag{1}$$

where $\sigma$ is the tensile stress in the adhesive, $\sigma_m$ the ultimate tensile strength of the adhesive, $E$ the initial Young's modulus and $\varepsilon$ the tensile strain in the adhesive.

Figure 3 shows the experimentally obtained tensile stress-strain relations of the adhesive using (ASTM D 638-89) as well as Equation (1). The shear strength and plastic characteristics of the epoxy adhesive were obtained by a bulk shear test. The method used for the bulk shear test of the epoxy adhesive is shown in Figure 4.

Figure 5 shows the shear stress-strain relations of the adhesive obtained from the bulk shear test of the adhesive and the multi-linear function calculated using the two-parameter nonlinear exponential Equation (1) and Poisson's ratio. Assuming that the nonlinear tensile property of the adhesive in an infinitesimal shear strain range was linear, the shear modulus of the adhesive was calculated using the elastic modulus and Poisson's ratio. Using the shear modulus of the adhesive calculated in the infinitesimal range, the shear stress-strain curve was obtained. Since the epoxy



TABLE I
Properties of the epoxy adhesive and the steel adherend

| | Adhesive (IPCO 9923) | Steel |
|---|---|---|
| Tensile modulus (GPa) | 1.30 | 207.0 |
| Poisson's ratio | 0.41 | 0.30 |
| Tensile strength (MPa) | 45.0 | not required |
| Shear strength (MPa) | 29.5 | not required |
| Shear strain limit | 0.60 | not required |
| C. T. E. ($10^{-6}$m/m°C) | 72.0 | 11.7 |
| Viscosity | paste type | not applicable |
| Cure temperature (°C) | 80.0 | not applicable |
| Cure time (hour) | 4 | not applicable |

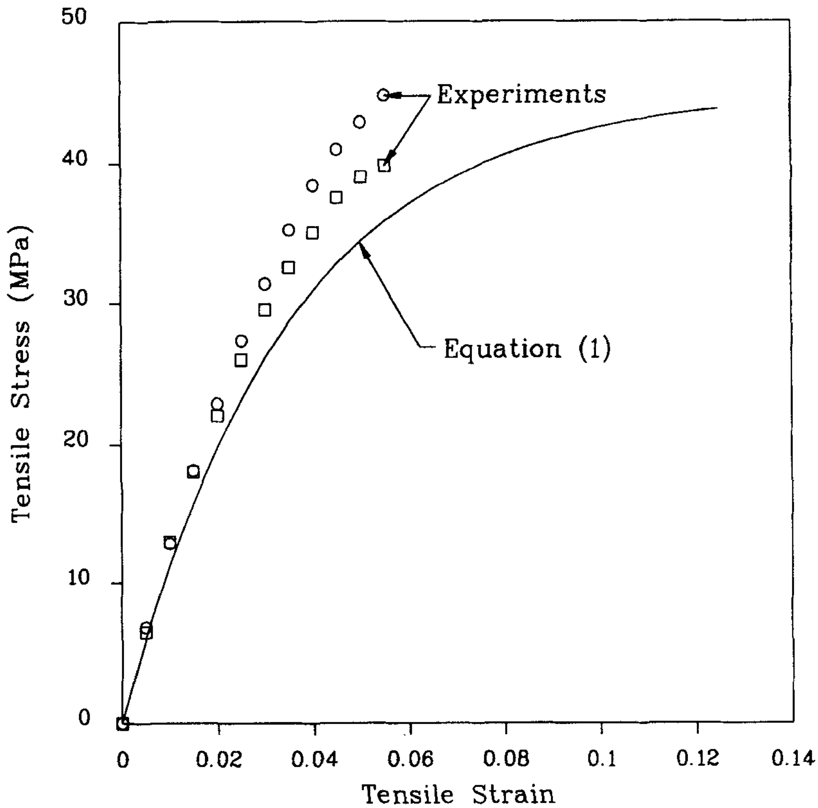


FIGURE 3 Tensile stress-strain relations of the epoxy adhesive (IPCO 9923).



adhesive used in this work was rubber-toughened, it revealed very large plastic strain, especially in the shear mode, as shown in Figure 5.

## STRESS ANALYSIS BY FINITE ELEMENT METHOD

Figure 6 shows the finite element mesh for stress analysis in which four-node isoparametric elements were used. The number of nodes was 1025 and the number of elements was 950. The tensile loads for the stress analysis of the adhesively-bonded joints were applied through the polynomial functions which were obtained by curve-fitting the experimental results.

Five elements were used uniformly along the adhesive layer thickness because the variation of the stresses was not large through the adhesive thickness.

Fifty elements were used along the adhesive layer length and the density of elements was increased towards to the edge of the adhesive taking into consideration the stress concentrations.

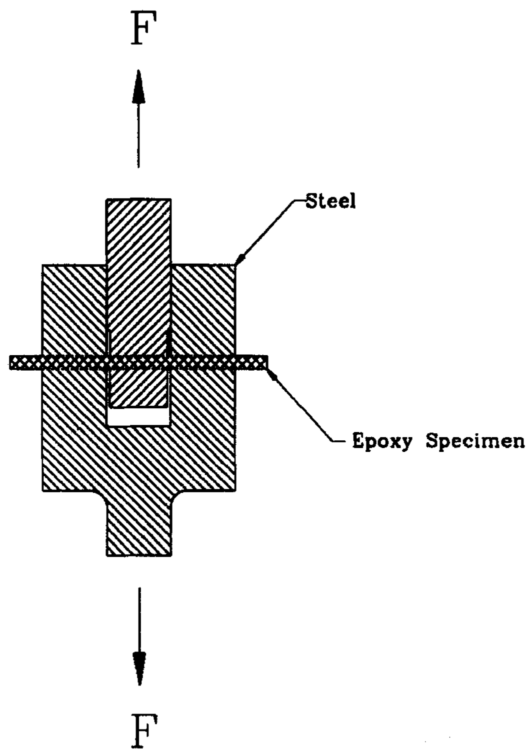


FIGURE 4 Bulk shear test of the epoxy adhesive.



In order to know the influences of the nonlinear mechanical property of the adhesive and the residual thermal stresses on the adhesive joints, the stress distributions of adhesively-bonded tubular single lap joints were calculated in four different cases of adhesive properties: (case 1) nonlinear mechanical property with residual thermal stresses of the adhesive, (case 2) linear mechanical property with residual thermal stresses of the adhesive, (case 3) nonlinear mechanical property without residual thermal stresses of the adhesive, and (case 4) linear mechanical property without residual thermal stresses of the adhesive.

The nonlinear mechanical property of the epoxy adhesive was modelled as Equation (1) and the linear property of the epoxy adhesive was modelled as 1.30 GPa in Table I.

The residual thermal stresses of the adhesive due to the temperature difference were calculated by using the coefficients of thermal expansion of the adherends and adhesive. The temperature difference between curing and testing $\Delta T$, was 60°C in (case 1) and (case 3), and was 0°C in (case 2) and (case 4) for the analysis of residual thermal stresses.

The coefficients of thermal expansion of the adherends and the epoxy adhesive between curing and testing were assumed to be linear.

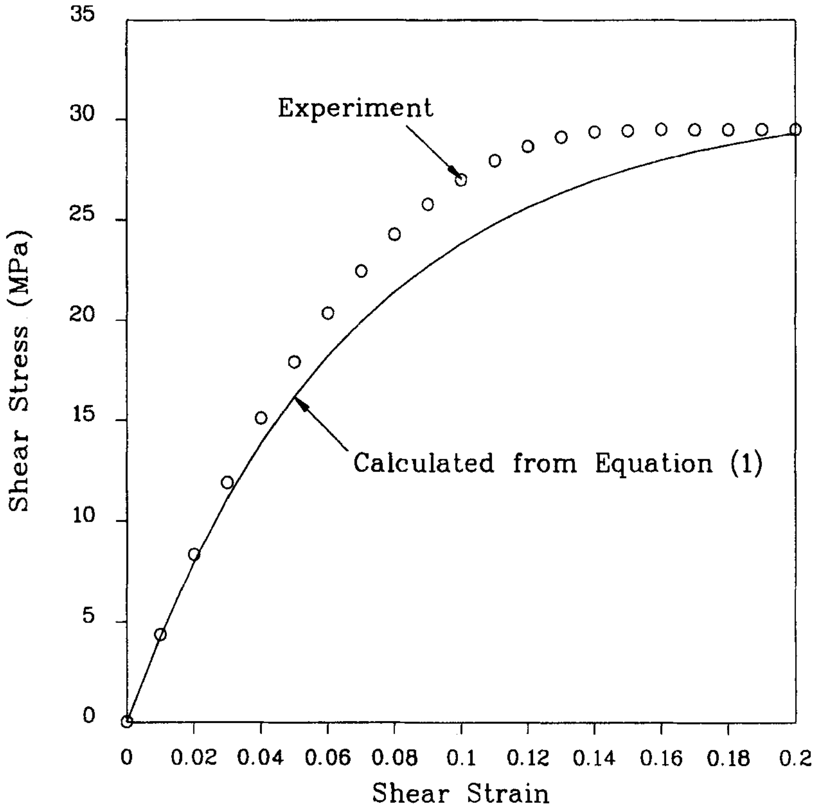


FIGURE 5 Shear stress-strain relations of the epoxy adhesive (IPCO 9923).

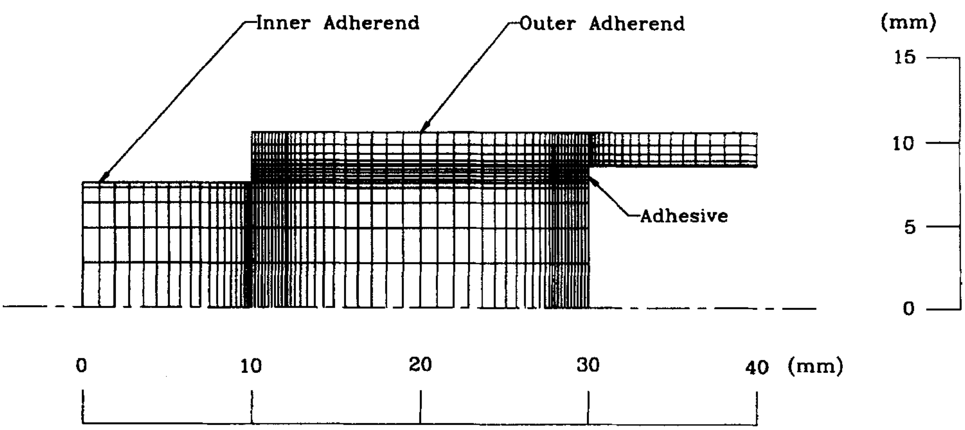


FIGURE 6 Finite element mesh for stress analysis.

Also, to know the effect of the initial residual thermal stresses on the adhesively-bonded joints, the initial residual thermal stresses originating from the temperature difference during the cure of the adhesive were calculated. The curing temperature of the adhesive joint was 80°C and the test temperature was 20°C.

## FAILURE MODEL OF ADHESIVE

It was assumed that the bonding strength between the adhesive and the adherend was not larger than the adhesive bulk shear strength because the residual thermal stresses were produced due to the temperature difference during the cure of adhesive. In the tensile experiments, the joint failures were found at the interface between the adhesive and the inner adherends. Therefore, the failure index in this analysis was applied at the adhesive elements which were in contact with the elements of the inner adherend.

In order to predict the failure condition of the adhesively-bonded joint, the non-dimensional failure index, $k$, was defined by the following equation.[13]

$$k = \sqrt{\left(\left(\frac{\sigma_{rr}}{S_T}\right)^2 + \left(\frac{\sigma_{\theta\theta}}{S_T}\right)^2 + \left(\frac{\sigma_{zz}}{S_T}\right)^2 + \left(\frac{\tau_{rz}}{S_S}\right)^2 + \left(\frac{\tau_{r\theta}}{S_S}\right)^2 + \left(\frac{\tau_{z\theta}}{S_S}\right)^2\right)} \tag{2}$$

where,

$S_T$ : bulk tensile strength of the adhesive
$S_S$ : bulk shear strength of the adhesive
$\sigma_{rr}$ : radial stress in adhesive
$\sigma_{\theta\theta}$: hoop stress in the adhesive
$\sigma_{zz}$: axial stress in the adhesive
$\tau_{rz}$ : shear stress in the adhesive
$\tau_{r\theta}$ : shear stress in the adhesive
$\tau_{z\theta}$ : shear stress in the adhesive

It was postulated that interfacial failure of the joint occurred when the failure index $k$ was equal to 1. Figure 7(a) shows the failure index of the adhesively-bonded joint when the adhesive thickness was 0.05 mm. In Figure 7, the failure indices are shown in four different case: (case 1) nonlinear mechanical property with residual thermal stresses of the adhesive, (case 2) linear mechanical property with residual thermal stresses of the adhesive, (case 3) nonlinear mechanical property without residual thermal stresses of the adhesive, and (case 4) linear mechanical property without residual thermal stresses of the adhesive.

Figure 7(b), 7(c) and 7(d) show the failure indices of the adhesive joints when the adhesive thicknesses were 0.1 mm, 0.5 mm, respectively. When the adhesive thicknesses were 0.05 mm and 0.1 mm, by comparing cases (1) and (3), it was found that the residual thermal stresses of fabrication affected the failure index little, while by comparing the cases (3) and (4) it was found that the linear and nonlinear mechanical

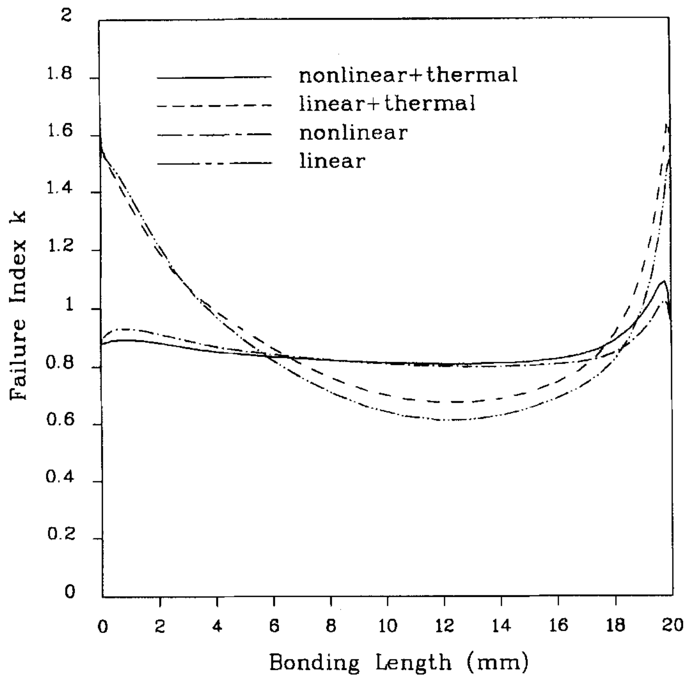

nonlinear+thermal
linear+thermal
nonlinear
linear
Failure Index k
Bonding Length (mm)
0
0.2
0.4
0.6
0.8
1
1.2
1.4
1.6
1.8
2
0
2
4
6
8
10
12
14
16
18
20


(7a)

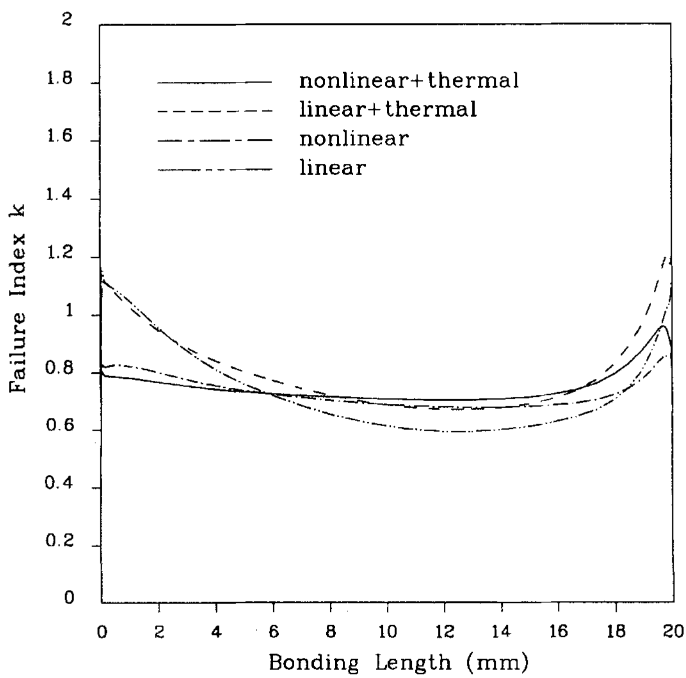

nonlinear+thermal
linear+thermal
nonlinear
linear
Failure Index k
Bonding Length (mm)
0
0.2
0.4
0.6
0.8
1
1.2
1.4
1.6
1.8
2
0
2
4
6
8
10
12
14
16
18
20


(7b)

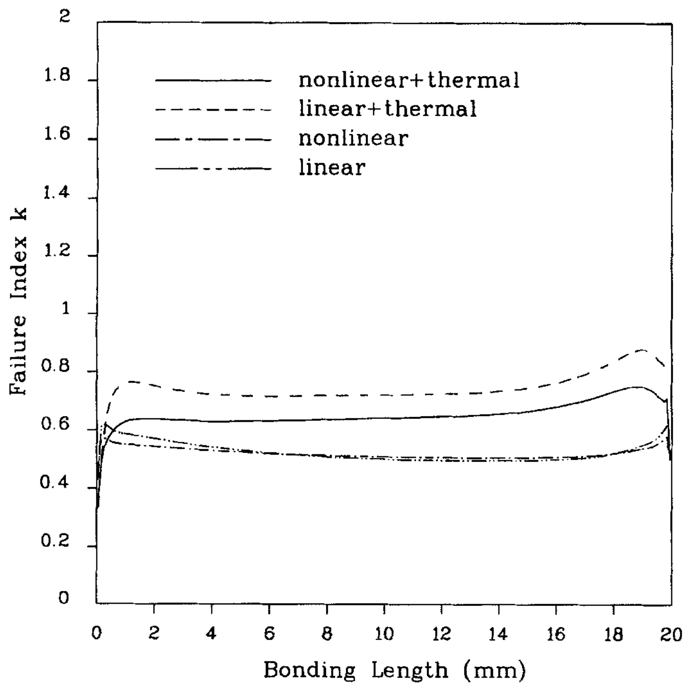


(7c)

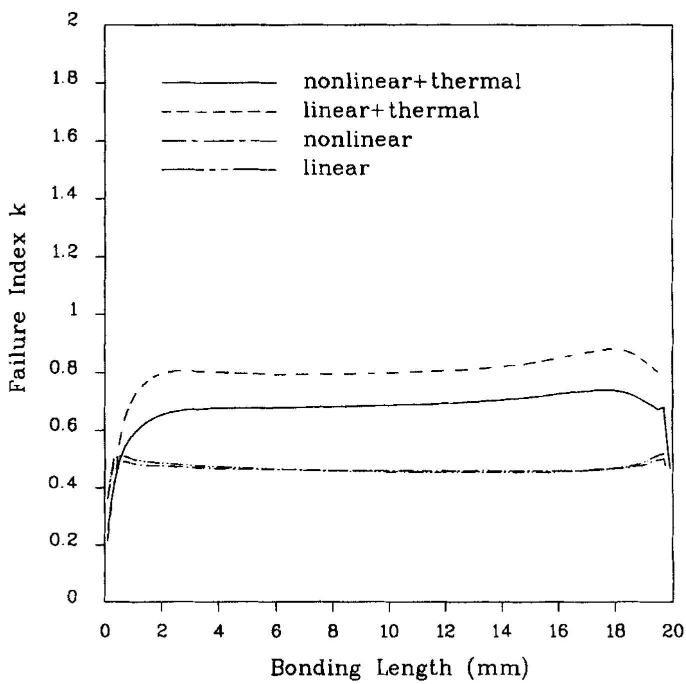


(7d)

FIGURE 7 Failure index, $k$, of the adhesively-bonded joint (a) 0.05 mm adhesive thickness (b) 0.1 mm adhesive thickness (c) 0.5 mm adhesive thickness (d) 1.0 mm adhesive thickness.

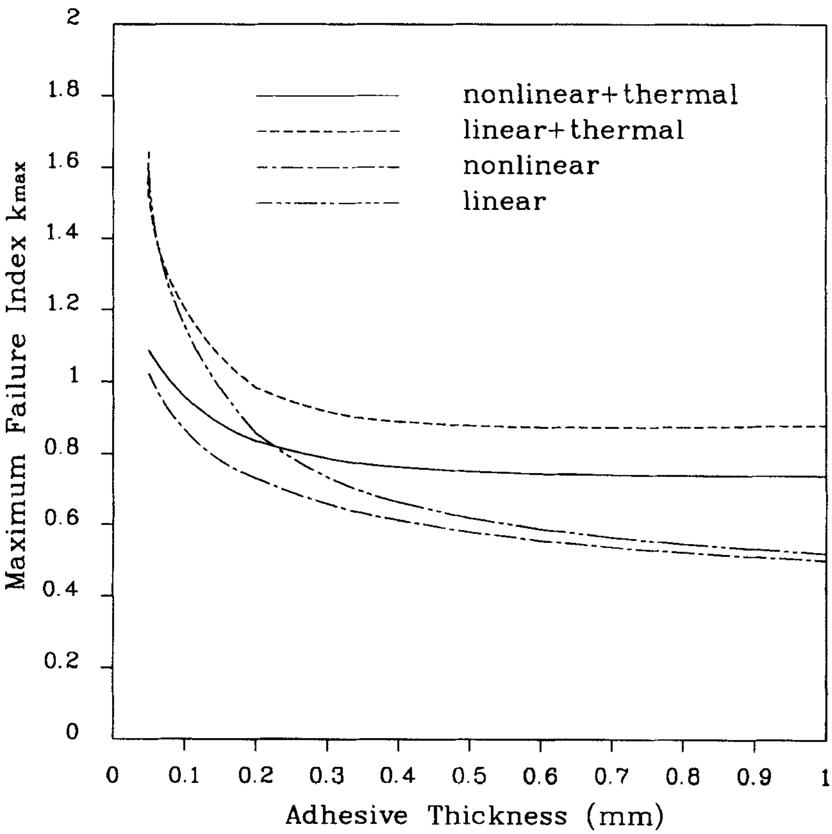


FIGURE 8 Maximum failure index, $k_{max}$, of the adhesively-bonded joint with respect to adhesive thickness.



properties affected the failure index much more. However, when the adhesive thicknesses were 0.5 mm and 1.0 mm, it was found that the residual thermal stresses of fabrication, rather than the linear and nonlinear mechanical properties, were more influential.

Figure 8 shows the variations of the maximum failure indices of the adhesive with respect to the adhesive thickness. The maximum indices occur along the bonding length of the joint. In Figure 8, the maximum failure index decreased rapidly up to 0.4 mm adhesive thickness, but was almost constant beyond that thickness. In Figure 8 the maximum failure index calculated with the linear mechanical property of the adhesive was larger than that calculated with the nonlinear property. Also, the index calculated with the residual thermal stress of fabrication in the adhesive was larger than that calcualted with no residual thermal stress of fabrication. Since the behavior of the adhesive was represented more precisely with the nonlinear mechanical property of the adhesive, it might be concluded that the maximum failure index with the nonlinear adhesive property was more reliable than that with the linear adhesive property.

Since it was found from the stress analysis of the joints that the maximum failure index with the residual thermal stresses of fabrication was larger than that without those stresses, the initial residual thermal stresses were calculated in order to investigate the influence of the thermal stresses of fabrication on the adhesively-bonded joints. From the calculated data of the initial residual thermal stresses, the initial failure index, $k_T$, was calculated as follows:

$$k_T = \sqrt{\left(\left(\frac{\sigma^T{}_{rr}}{S_T}\right)^2 + \left(\frac{\sigma^T{}_{\theta\theta}}{S_T}\right)^2 + \left(\frac{\sigma^T{}_{zz}}{S_T}\right)^2 + \left(\frac{\tau^T{}_{rz}}{S_S}\right)^2\right)} \quad (3)$$

where,
$S_T$ : bulk tensile strength of the adhesive
$S_S$ : bulk shear strength of the adhesive
$\sigma^T_{rr}$ : radial residual thermal stress in the adhesive
$\sigma^T_{\theta\theta}$: hoop residual thermal stress in the adhesive
$\sigma^T_{zz}$: axial residual thermal stress in the adhesive
$\tau^T_{rz}$ : shear resudial thermal stress in the adhesive

Figure 9 shows the initial failure index, $k_T$, with respect to the adhesive thickness calculated using Equation (3). In Figure 9, the initial failure index, $k_T$, increased as

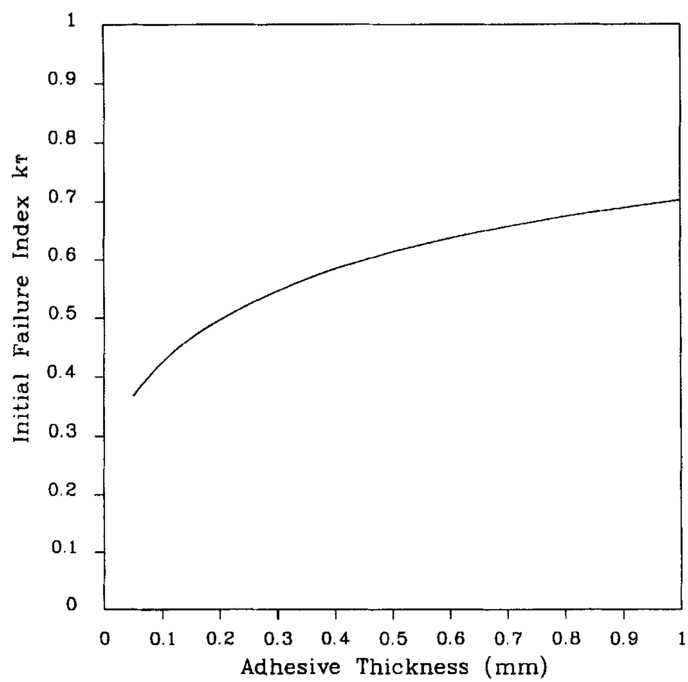


FIGURE 9 Initial failure index, $k_T$, of the adhesively-bonded joint by residual thermal stresses of fabrication with respect to adhesive thickness.

the adhesive thickness increased. The increase of $k_T$ was caused by increases of all the stress components, especially of the peel component of stress in Equation (3).

However, the slope of $k_T$ was decreased as the adhesive thickness was increased. Since the maximum failure index, $k_{max}$, and the initial failure index, $k_T$, have opposite slopes, in this work, it was found that they could be related as follows.

$$k_{max}^2 + k_T^2 \approx 1 \tag{4}$$

where $k_{max}$ represents the maximum failure index calculated taking into account the nonlinear mechanical property of the adhesive with residual thermal stresses.

From the relationship of Equation (4), the practical fracture index, $k_F$, was defined as follows:

$$k_F \equiv \sqrt{1 - k_T^2} \tag{5}$$

Figure 10 shows the maximum failure index, $k_{max}$, and the practical fracture index, $k_F$, calculated when the maximum tensile load bearing capabilities of the adhesively-bonded joints obtained from the static tensile tests were applied to the joints. From Figure 10, it was found that the value of the practical fracture index, $k_F$, was almost the same as the maximum failure index, $k_{max}$, calculated taking into account the nonlinear property of the adhesive with the residual thermal stresses of fabrication.



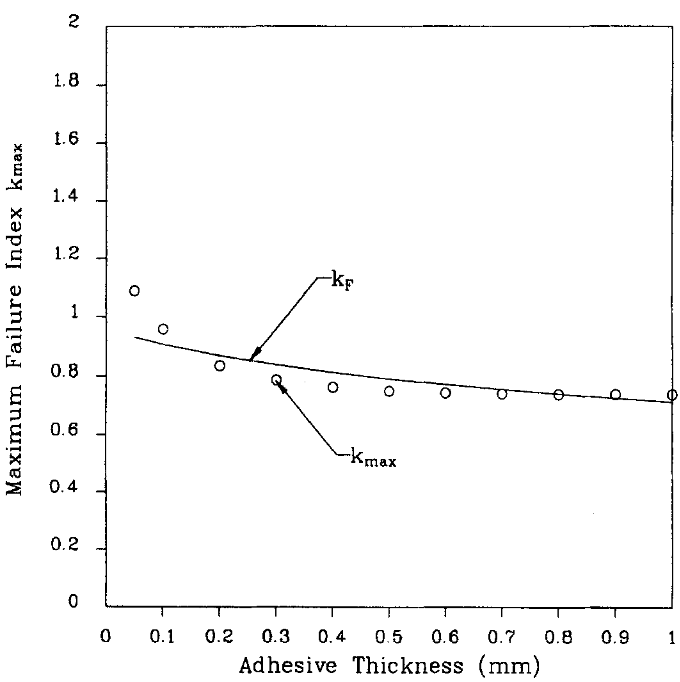


FIGURE 10 Maximum failure index, $k_{max}$, and practical fracture index, $k_F$, of the adhesively-bonded joint with respect to adhesive thickness.

Therefore, it was postulated that the fracture of the adhesively-bonded joints occurred when $k_{max}$ was equal to $k_F$.

From these results, it was found that the finite element analysis with the nonlinear mechanical property of the adhesive with the fabrication residual thermal stresses must be used in order to calculate the stress distribution of the adhesively-bonded tubular single lap joint more accurately. Also, it was found that to predict accurately the static tensile strength of the joint, the practical fracture index, $k_F$, which takes into consideration the reduction of the fracture strength of the adhesive due to the residual thermal stresses of fabrication must be calculated.

## CONCLUSIONS

In this work, the tensile load-bearing capabilities of the adhesively-bonded tubular single lap joints with steel-steel adherends were tested with respect to the adhesive thickness. From the tests, it was found that the tensile load-bearing capabilities were decreased as the adhesive thickness was increased.

The stress distributions of the adhesively-bonded joints were calculated when the tensile load-bearing capabilities of the joint obtained from the static tensile tests were applied.

Then the practical fracture index was calculated, taking into account the nonlinear mechanical properties of the adhesive and the residual thermal stresses of fabrication.

From the calculated data, the failure model for the adhesively-bonded tubular single lap joints was proposed: since the practical fracture index, $k_F$, was almost the same as the maximum failure index, $k_{max}$, calculated with the nonlinear property of the adhesive and residual thermal stresses of fabrication, it was postulated that the fracture of the adhesively-bonded joints occurred when $k_{max}$ was equal to $k_F$.



### Acknowledgements

This research was financially supported by the Korea Ministry of Science and Technology under international collaboration research between the Korea Advanced Institute of Science and Technology and FRAMASOFT of France.

### References

1. P. K Mallick, *Fiber-Reinforced Composites*, (Marcel Dekker, Inc., New York and Basel), pp. 417–425 (1988).
2. A. J. Kinloch, *Adhesion and Adhesives*, (Chapman and Hall Ltd., New York), pp. 2–3 (1987).
3. J. L. Lubkin and E. Reissner, "Stress distribution and design data for adhesive lap joints between circular tubes," *J. Appl. Mechanics, Trans. ASME*, **78**, 1213–1221 (1956).
4. R. D. Adams and N. A. Peppiatt, "Stress analysis of adhesive bonded tubular lap joints," *J. Adhesion*, **9**, 1–18 (1977).
5. S. A. Griffiin, S. S. Pang and C. Yang, "Strength model of adhesive bonded composite pipe joints under tension," *Polym. Eng. and Sci.*, **31**(7), 533–538 (1991).
6. Y. P. Shi and S. Cheng, "Analysis of adhesive-bonded cylindrical lap joints subjected to tensional load," *J. Eng. Mechanics*, **119**(3), 584–602 (1993).

7. L. P. Terekhova and I. A. Skoryi, "Stresses in Bonded joints of Thin Cylindrical Shells,"*Strength Mat.*, **4**, 1271–1274 (1979).
8. N. M. Kukovyakin and I. A. Skoryi, "Estimating the Strength of Bonded Cylindrical Joints," *Russian Eng. J.*, **52**(4), 40–43 (1972).
9. N. L. Harrison and W. J. Harrison, "The Stresses in an Adhesive Layer," *J. Adhesion*, **3**, 195–212 (1972).
10. T. A Osswald and J. Rietveld, "Measuring Constitutive Properties," in *Adhesives and Sealants*, (ASM International, Metals Park, Ohio), pp. 315–316 (1990).
11. F. L. Matthews, *Joining Fiber-reinforced Plastics*, (Elsevier Applied Science, London and New York), pp. 185–226 (1986).
12. D. G. Lee, K. S. Kim and Y. T. Lim, "An Experimental Study of Fatigue Strength for Adhesively Bonded Tubular Single Lap Joints," *J. Adhesion*, **35**, 39–53 (1991).
13. S. J. Lee and D. G. Lee, "Development of a Failure Model for the Adhesively Bonded Tubular Single Lap Joint," *J. Adhesion*, **40**, 1–14 (1992).